

## Higher harmonic generation at metal surfaces by powerful bichromatic laser fields

S. Varró

*Research Institute for Solid State Physics of the Hungarian Academy of Sciences, P. O. Box 49, H-1525 Budapest, Hungary*

F. Ehlötzky

*Institute for Theoretical Physics, University of Innsbruck, Technikerstrasse 25, A-6020 Innsbruck, Austria*

(Received 2 January 1997; revised manuscript received 24 April 1997)

We generalize our recent model calculations on the generation of higher harmonics at metal surfaces by a powerful femtosecond laser pulse [Phys. Rev. A **54**, 3245 (1996)] for the case in which a bichromatic field of frequencies  $\omega$  and  $2\omega$  is applied, where both components are out of phase by an angle  $\phi$ , and we discuss the coherent phase control of the harmonic generation process, relating our results to those obtained for harmonic generation by shining a bichromatic laser field on atoms. [S1050-2947(97)00809-3]

PACS number(s): 79.20.Ds, 32.80.Wr, 42.50.Hz

Some time ago, it was suggested to coherently control laser-induced molecular reactions by applying a bichromatic laser field of commensurable frequencies, the relative phase of which can be conveniently tuned [1]. Since then, this idea has been employed in various branches of multiphoton physics, among others in multiphoton above threshold ionization (ATI) of atoms [2] and in the concomitant harmonic generation (HG) [3]. The recent advance in the production of very powerful femtosecond laser pulses made it possible to generate very high harmonics by shining laser light of some  $10^{17}$  W/cm<sup>2</sup> at grazing incidence on solid surfaces, in particular on metals, as documented by two new experiments [4,5]. To explain these highly nonlinear effects, two model calculations have been presented recently [6,7], of which our model [7] reproduced the experimental data surprisingly well.

It is the purpose of the present short paper to adapt our model to the generation of harmonics at metal surfaces in a bichromatic field of frequencies  $\omega$  and  $2\omega$  and investigate the harmonic rates as a function of the relative phase  $\phi$  of the two field components. We do not intend to reproduce all the details of our theory here, except putting down some of the essentials and referring for the rest to our foregoing work [7].

We assume that both components of the bichromatic field have the same linear polarization  $\vec{\epsilon}$  and consider grazing incidence of the laser light onto the metal surface such that  $\vec{\epsilon}$  is very close to the normal  $\vec{e}_z$  onto the surface (i.e., we choose  $p$  polarization). Since the surface plasma, generated by the powerful laser pulse, has a thickness less than a laser wavelength we may safely describe the laser field in dipole approximation and choose the bichromatic field in the form

$$\vec{E}(t) = \vec{\epsilon}[F_0^1 \sin \omega t + F_0^2 \sin(2\omega t + \phi)], \quad (1)$$

where  $F_0^1$  and  $F_0^2$  are the field strengths of the two components. With this choice, and in the idealized case that  $\vec{\epsilon} = \vec{e}_z$ , we get for the space-translated potential of the Sommerfeld model of the solid embedded in the two fields [7]

$$V[z + \alpha_0^1 \sin \omega t + \alpha_0^2 \sin(2\omega t + \phi)] = V_0[\theta(z + \alpha_0^1 \sin \omega t + \alpha_0^2 \sin(2\omega t + \phi)) - 1], \quad (2)$$

where  $\alpha_0^i = eF_0^i/m(i\omega)^2$ , with  $i=1,2$ ,  $V_0 = E_F + W$  is the

depth of the potential step, and  $\theta(z)$  is the step function. For the evaluation of the transition matrix element  $T_n$  for the  $n$ th harmonic we need to evaluate

$$\begin{aligned} & \vec{\nabla}_z V[z + \alpha_0^1 \sin \omega t + \alpha_0^2 \sin(2\omega t + \phi)] \\ &= \sum_n \vec{\nabla}_z V_n(z) \exp(-in\omega t), \end{aligned} \quad (3)$$

where  $\vec{\nabla}_z V_n(z)$  is obtained from Eq. (2) to be given by

$$\vec{\nabla}_z V_n(z) = V_0(2\pi)^{-1} \int dk \exp(-ikz) B_n(k\alpha_0^1; k\alpha_0^2; \phi), \quad (4)$$

in which  $B_n$  is a generalized Bessel function defined by

$$B_n(k\alpha_0^1; k\alpha_0^2; \phi) = \sum_{\ell} J_{n-2\ell}(k\alpha_0^1) J_{\ell}(k\alpha_0^2) \exp(-i\ell\phi). \quad (5)$$

Consequently, we get for our transition matrix element of harmonic generation [7]

$$T_n = -2\pi i \delta(E' + \hbar\omega' - E - n\hbar\omega) \langle \vec{k}' | \vec{\epsilon}' \cdot \vec{\epsilon} \partial_z V_n(z) | \vec{k} \rangle \quad (6)$$

in which  $|\vec{k}\rangle$  and  $|\vec{k}'\rangle$  are free electron states of the electrons of the surface plasma which scatter at the oscillating potential well. Inserting in Eq. (6) from Eqs. (4) and (5) the expression for  $\vec{\nabla}_z V_n(z)$  we find

$$\begin{aligned} & \vec{\epsilon}' \cdot \vec{\epsilon} \langle \vec{k}' | \partial_z V_n(z) | \vec{k} \rangle \\ &= \vec{\epsilon}' \cdot \vec{\epsilon} \delta_{k_x, k'_x} \delta_{k_y, k'_y} V_0 L^{-1} B_n((k_z - k'_z)) \\ & \quad \times \alpha_0^1; (k_z - k'_z) \alpha_0^2; \phi), \end{aligned} \quad (7)$$

where  $\vec{\epsilon}'$  is the polarization vector of the spontaneously emitted harmonic field. Following along the lines of our foregoing work [7], we get, after evaluation of the transition probabilities from Eqs. (6) and (7) and integration over the Fermi distributions for the free and occupied electron states of the degenerate electron gas, the following expression for

the differential production rates per unit surface element of harmonic frequencies  $\omega' = n\omega$  ( $n=2,3,4,\dots$ ) in the bichromatic field

$$dw_n/d\Omega = C(V_0, T, \omega)(\vec{\epsilon}' \cdot \vec{\epsilon})^2 R_n/n$$

$$R_n = \int_0^\infty (dy/y) \{ \exp[b(y^2-1)] + 1 \}^{-1} B_n^2(a_1 y; a_2 y; \varphi), \quad (8)$$

where  $C$  is a normalization constant which we do not need to consider since in all available experimental data only relative harmonic rates are presented. Hence we shall concentrate in the following discussion on the relevant term  $R_n/n$ . In Eq. (8) we have introduced the dimensionless parameters

$$a_i = 2k_F \alpha_0^i = 2k_F e F_0^i / m(i\omega)^2, \quad (9)$$

$$i = 1, 2$$

$$b = E_F / k_B T, \quad (\hbar k_F)^2 / 2m = E_F,$$

where  $E_F$  is the Fermi energy,  $k_B$  Boltzmann's constant, and  $T$  the absolute temperature. As indicated in our foregoing work, the parameters  $a_i$  are, however, not the effective parameters. First, we have to multiply these by a factor  $2\sin\theta$ , since in an actual experiment the laser polarization is not exactly perpendicular onto the solid surface for the laser beam impinges under an angle  $\theta$  with respect to the normal, and, secondly, we have to observe that the effective laser field strengths  $F_0^i$  in the surface plasma are related to the incoming external fields  $F_e^i$  by the appropriate boundary conditions  $\epsilon_i F_0^i = F_e^i$  with  $\epsilon_i = 1 - \omega_p^2 / (i\omega)^2$  being the dielectric constants of the two fields. Since, however, for the very dense surface plasma  $\omega_p \gg \omega$  we get for the field strengths inside the plasma the reduction factors  $F_0^i = -[(i\omega)^2 / \omega_p^2] F_e^i$ . Consequently, the effective parameters  $a_{\text{eff}}^i$  to be used in Eq. (8) are given by

$$a_{\text{eff}}^i = 2[(i\omega)^2 / \omega_p^2] a_i \sin\theta, \quad i = 1, 2. \quad (10)$$

For the following numerical examples we choose the data of the experiment of von der Linde *et al.* [5]. They used a Ti:sapphire laser with  $\hbar\omega = 1.56$  eV ( $\omega = 2.5 \times 10^{15}$  sec $^{-1}$ ) which will be our fundamental field of intensity  $I = 10^{17}$  W/cm $^2$  and 100-fs pulse duration. As a target was taken aluminum with  $E_F = 11.7$  eV and an electron density of  $n = 18.1 \times 10^{22}$  cm $^{-3}$  (which is roughly the density of the surface plasma) so that the plasmon energy is  $\hbar\omega_p = 15.82$  eV ( $\omega_p = 2.41 \times 10^{16}$  sec $^{-1}$ ). Moreover, in this experiment  $\theta = 68^\circ$ . Then, with the above relations, the effective parameter for the fundamental field will be given by  $a_{\text{eff}}^1 = 16.015$ . If we choose for the second field a field strength  $F_0^2 = F_0^1/4$ , corresponding to an intensity of the second field of  $I_2 = 6.3 \times 10^{15}$  W/cm $^2$ , then we find that the effective parameter of the second field is given by  $a_{\text{eff}}^2 = a_{\text{eff}}^1/4$ . In this case the second Bessel function in  $B_n$  still yields a considerable contribution, although the intensity of the second field is lower by about two orders of magnitude. As we have shown in our foregoing work, for a single laser frequency the cutoff  $n_c$  of the harmonic spectrum is roughly determined by  $a_{\text{eff}}^1$ , which

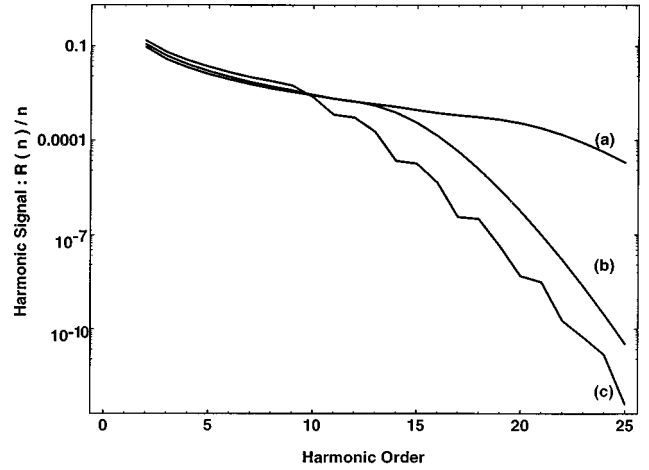


FIG. 1. Presents  $R_n/n$  in a bichromatic field for (a)  $\varphi=0$  and (c)  $\varphi=\pi$  to be compared with (b) for a single frequency. While for  $\varphi=0$  many more higher harmonics appear than for a single frequency, the cutoff of the spectrum for  $\varphi=\pi$  is at a lower value of  $n$  than for a single frequency but the harmonic rates are enhanced at small  $n$ . The power of the fundamental field is  $10^{17}$  W/cm $^2$  and of the second field  $6.3 \times 10^{15}$  W/cm $^2$ .

is in quite good agreement with the experimental findings of von der Linde *et al.* [5]. In the case of the bichromatic field, this cannot be so, since here the cutoff will strongly depend on the relative phase of the two fields, which determines the maximum values of the generalized Bessel functions  $B_n$ . This phase dependence of the cutoff will be clearly seen in our figures below. Since the harmonics at the surface of the metal can only be generated as long as the surface plasma has not been heated up, which means that all the energy supplied by the laser pulse has been transformed into thermal energy, we assume that initially the plasma is cold, i.e., at room temperature ( $T=300$  K,  $k_B T=0.025$  eV). In this case we find for the second parameter in Eq. (9) the value  $b=468$ . Temperatures up to about  $k_B T=5$  eV are still permissible. Beyond that value the time  $\tau_c$  between two electron collisions becomes shorter than the laser period  $T$  and thus no electron oscillations in the laser field can take place any longer. As we have seen in our foregoing work, for sufficiently low temperatures of a few  $k_B T$  the harmonic spectrum is almost temperature independent up to the cutoff. Hence we do not discuss the temperature dependence here.

In the following figures we discuss the  $\varphi$  dependence of  $R_n/n$  as a function of the harmonic order  $n$  in the range  $0 \leq \varphi \leq \pi$  for a few selected values and compare the data with those for a single frequency.

Figure 1 shows the harmonic rates  $R_n/n$  in a bichromatic field as a function of the nonlinear order  $n$  for (a)  $\varphi=0$  and (c)  $\varphi=\pi$  to be compared with (b) for a single frequency when the second field is turned off. In both cases the fundamental field has the same intensity of  $10^{17}$  W/cm $^2$  while the second field has the intensity of  $6.3 \times 10^{15}$  W/cm $^2$ . As is apparent, for  $\varphi=0$  many more higher harmonics are generated than with a single frequency laser pulse. This happens though the second field has a considerably lower intensity. On the other hand, for  $\varphi=\pi$  destructive interferences in the evaluation of the generalized Bessel functions  $B_n$  lead to higher harmonic signals at small harmonic orders but to a

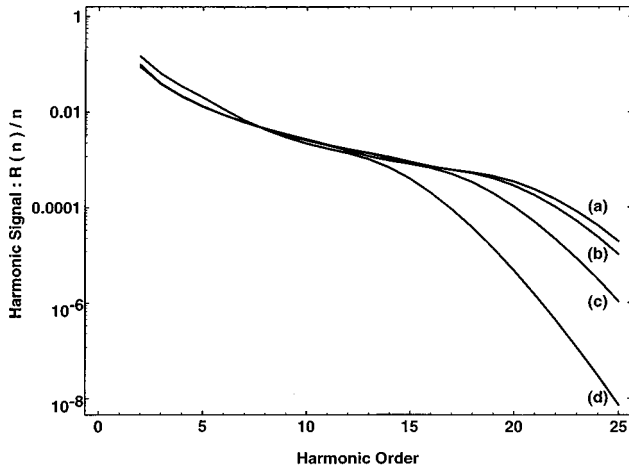


FIG. 2. Shows the decrease of the number of harmonics generated with increasing  $\varphi$  for (a)  $\varphi=0$ , (b)  $\varphi=\pi/4$ , (c)  $\varphi=\pi/2$ , and (d)  $\varphi=3\pi/4$ . Here too one recognizes the features already apparent in Fig. 1, such as the enhancement of the harmonic rates for small  $n$  with increasing phase  $\varphi$ .

less extended spectrum. Since the analytic properties of the generalized Bessel functions are rather involved and not so well known, it is hard to find a simple argument for the results of the above interference effects. The following fact may, however, be the reason for the above effects. If we replace in the definition (5) of the generalized Bessel functions the phase  $\varphi=0$  by  $\varphi=\pi$ , then the various terms of the sum over  $\ell$  will alternate in sign due to the factor  $\exp(-i\ell\pi)=(-1)^\ell$ . Hence, for the case  $\varphi=0$  there appear to be more constructive interferences than for the case  $\varphi=\pi$ . But this cannot be the only reason.

Figure 2 presents even more clearly the decrease of the order  $n$  of harmonics generated with increasing relative phase  $\varphi$  for (a)  $\varphi=0$ , (b)  $\varphi=\pi/4$ , (c)  $\varphi=\pi/2$ , and (d)  $\varphi=\pi$ , while on the other hand there is an indication of the increase of the harmonic rates at small harmonic orders with increasing value of the phase.

This increase of the harmonic rates at small values of the nonlinear order and simultaneous decrease at large  $n$  for increasing values of the phase is drastically demonstrated in Fig. 3, where the relative rates  $R_n(\varphi)/R_n(\varphi=0)$  are plotted as a function of  $n$  for (a)  $\varphi=\pi/4$ , (b)  $\varphi=\pi/2$ , (c)  $\varphi=3\pi/2$ , and (d)  $\varphi=\pi$ . This figure also shows very nicely the decrease of the cutoff value of the harmonic spectrum with increasing phase. It is interesting to observe that all curves intersect at roughly the same value of  $n$  somewhere between 8 and 10. This can also be seen, though it is less pronounced, in Figs. 1 and 2. As pointed out above, due to the complex structure of the generalized Bessel functions it is hard to find a simple explanation for this feature.

The changes between the harmonic rates for a single frequency, denoted by  $S_n/n$ , and for a bichromatic field,  $R_n/n$ , are particularly dramatic for  $\varphi=\pi$ . This is shown in Fig. 4, where  $S_n/R_n(\varphi=\pi)$  is plotted on the large scale and its inverse,  $R_n(\varphi=\pi)/S_n$ , is presented in the inset.

Our formula for the harmonic rates  $R_n/n$  has a simple intuitive interpretation. The generalized Bessel function  $B_n^2(a_{\text{eff}}^1 y; a_{\text{eff}}^2 y; \varphi)$  describes the probability of harmonic generation by raising an electron from a particular energy level

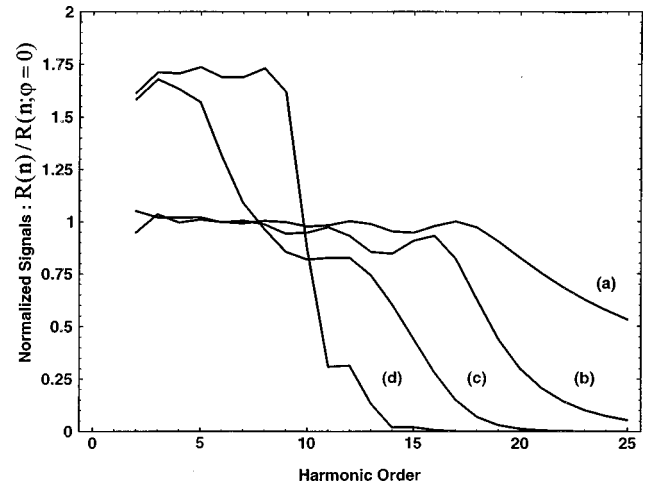


FIG. 3. Demonstrates more drastically the increase of  $R_n/n$  at small  $n$  by presenting  $R_n(\varphi)/R_n(\varphi=0)$  for (a)  $\varphi=\pi/4$ , (b)  $\varphi=\pi/2$ , (c)  $\varphi=3\pi/4$ , and (d)  $\varphi=\pi$ . Simultaneously one recognizes the decrease of the cutoff frequency.

of the Fermi distribution into the continuum by absorbing  $n$  photons  $\hbar\omega$  from the two fields and by then falling back to the same level, thereby emitting a harmonic quantum  $n\hbar\omega$ . All these probabilities are then summed up over all available levels of the Fermi distribution to yield the total production rates. This picture is in fact very similar to the simple picture of harmonic generation by atoms. But we have to remind ourselves that atoms in their ground state are spherically symmetric systems so that due to parity conservation only odd harmonics are generated, whereas a solid surface does not have this symmetry and hence even and odd harmonics are produced. On the other hand, the polarization dependence in both cases is the same, namely  $(\vec{\varepsilon}' \cdot \vec{\varepsilon})^2$ . Therefore it is not surprising that similar features as discussed above for harmonic generation in a bichromatic field, like the decrease of the harmonic spectrum with increasing relative phase  $\varphi$  and the simultaneous increase of the harmonic rates

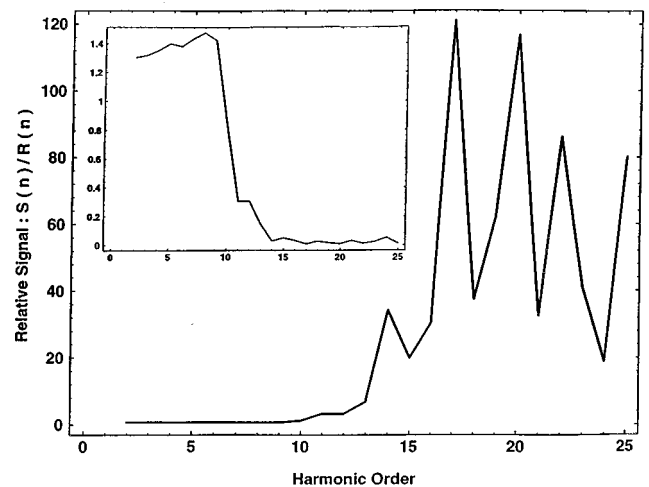


FIG. 4. Shows on a large scale  $S_n/R_n(\varphi=\pi)$  and in the inset  $R_n(\varphi=\pi)/S_n$ , where  $S_n$  are the rates for a single frequency. While the inset drastically demonstrates the early cutoff of the spectrum for  $\varphi=\pi$ , the large scale figure shows for higher  $n$  the zigzagging of the harmonic rates for  $\varphi=\pi$  which are already apparent in Fig. 1.

at small harmonic orders, are also met if this process is considered for atoms [3]. One final remark might be in order. In our model of harmonic generation at a metal surface the cutoff law is not determined by  $W+3U_p$  where  $W$  is the work function, representing here the ionization energy, and  $U_p$  is the ponderomotive energy. This law was found to hold for atoms [8] but would predict here an enormously extended harmonic spectrum which is not observed. Probably this has something to do with a rather high ionization probability at the metal surface which we have not investigated here. There is also another reason why apparently the production efficiency of harmonics at solid surfaces is not so high as one might expect on account of the high electron density of the surface plasma. Since the electron gas is degenerate, only a fraction  $k_B T/E_F$  of the electron density will be available for the generation process and this reduces the effective density of electrons at room temperature to  $n_e^{\text{eff}}=4\times 10^{20}\text{ cm}^{-3}$ . On the other hand, the laser interaction volume on the solid surface is about  $5\times 10^{-6}\text{ cm}^3$  so that the number of electrons available per laser shot is about  $2\times 10^{17}$ . This is then of a similar order of magnitude as one meets in a gas jet which is crossed by the laser beam.

Summarizing, we have demonstrated by using a straightforward extension of our model for the generation of harmonics at metal surface [7] for the case of a bichromatic field of frequencies  $\omega$  and  $2\omega$  the following main features:

(a) For a laser intensity of the fundamental field of  $10^{17}\text{ W/cm}^2$  and for the second field of  $6.3\times 10^{15}\text{ W/cm}^2$  the spectrum of harmonics will extend to much higher nonlinear orders for the phase  $\varphi=0$  than is observed for a single field [5] and (b) for larger values of the relative phase the cutoff of the spectrum gets decreased while the harmonic rates are increased at the same time.

Despite the differences between the harmonic generation by atoms and at metal surfaces, these two processes appear to have the above two features (a) and (b) in common if harmonic generation takes place in a bichromatic field.

This work has been supported by the East-West Program of the Austrian Academy of Sciences and by the Austrian Ministry of Science, Research, Art and Transportation under Contract No. 45.372/4-IV3/95 as well as by the Hungarian National Science Foundation (OTKA) under Project No. R.T016140.

- 
- [1] M. Shapiro, J. W. Hepburn, and P. Brumer, *Chem. Phys. Lett.* **149**, 451 (1988).
- [2] C. E. Chen, Y. Y. Yin, and D. S. Elliott, *Phys. Rev. Lett.* **64**, 507 (1990); D. W. Schuhmacher, F. Weihe, H. G. Muller, and P. H. Bucksbaum *ibid.* **73**, 1344 (1994); B. Sheehy, B. Walker, and L. F. DiMauro, *ibid.* **74**, 4799 (1995).
- [3] A. Sanpera, J. B. Watson, M. Lewenstein, and K. Burnett, *Phys. Rev. A* **54**, 4320 (1996); D. B. Milošević and B. Piraux, *ibid.* **54**, 1522 (1996); I. Mercer, E. Mevel, R. Zerne, A. L'Huillier, P. Antoine, and C.-G. Wahlström, *Phys. Rev. Lett.* **77**, 1731 (1996); D. A. Telnov, J. Wang, and S.-I. Chu, *Phys. Rev. A* **52**, 3988 (1995); M. Protopapas, A. Sanpera, P. L. Knight, and K. Burnett, *ibid.* **52**, R2527 (1995); S. Long, W. Becker, and J. K. McIver, *ibid.* **52**, 2262 (1995); M. Protopapas, P. L. Knight, and K. Burnett, *Phys. Rev. A* **49**, 1945 (1994); M. D. Perry and J. K. Crane, *ibid.* **48**, R4051 (1993).
- [4] S. Kohlweyer, G. D. Tsakiris, C.-G. Wahlström, C. Tillman, and I. Mercer, *Opt. Commun.* **117**, 431 (1995).
- [5] D. von der Linde, T. Engers, G. Jenke, P. Agostini, G. Grillon, E. Nibbering, A. Mysyrovicz, and A. Antonetti, *Phys. Rev. A* **52**, R25 (1995).
- [6] R. Lichters, J. Meyer-ter-Vehn, and A. Pukhov, *Phys. Plasmas* **3**, 3425 (1996).
- [7] S. Varró and F. Ehlotzky, *Phys. Rev. A* **54**, 3245 (1996).
- [8] J. L. Krause, K. J. Schafer, and K. C. Kulander, *Phys. Rev. Lett.* **68**, 3535 (1992).